Suppressing Undesired Echoes by Sparsity Based Time Gating of Reconstructed Sources

Josef Knapp, Jonas Kornprobst, Thomas F. Eibert,
Chair of High-Frequency Engineering, Department of Electrical and Computer Engineering,
Technical University of Munich, 80290 Munich, Germany, josef.knapp@tum.de

***Abstract*—The free-space radiation characteristic of an antenna under test (AUT) is determined from measurements in proximity of a scatterer by time gating reconstructed equivalent currents for the AUT and the scatterer. The presented approach effectively combines spatial filtering methods with time domain methods while mitigating their individual drawbacks. In contrast to conventional time-gating methods which usually work on the measured probe signals this approach allows to get rid of undesired echo perturbations even if measurement samples are located in the shadow region of the scatterer and the line of sight (LOS) contribution and the echo contribution are indistinguishable for the field probe. In contrast to conventional frequency domain methods, mutual coupling contributions of the AUT currents are identified and removed in the time domain representation of the reconstructed currents. Numerical examples show that, due to the sparse time domain representation of the currents, the free-space radiation of the AUT can be determined accurately even at the borders of the measured bandwidth.**

***Index Terms*—antennas, electromagnetics, propagation, measurements.**

I. Introduction

When one measures the radiated field of an antenna under test (AUT), the interest usually lies in the free-space radiation characteristic, i.e., the radiated fields of the AUT as if it was solely placed in free space without any (scattering) objects surrounding it. To emulate this scenario, anechoic antenna measurement chambers are equipped with absorbers on all surfaces within the chamber to avoid distortions in the measured signals from undesired scattering. Additionally, the antenna is mounted carefully such that the mounting structures have as little impact on the antenna radiation behavior as possible. Unfortunately, these measures are not perfect and even the most carefully planned measurement setup changes the measured fields with respect to the ideal case.

After the measurements have been obtained, one can get rid of certain echo perturbations by post-processing techniques. These post-processing techniques can also have advantages for simulated data. When the AUT is simulated in certain environmental conditions (e.g., in proximity of a reflective wall), the current distribution on the antenna may be different from the one in free-space. If the deviation of the current distribution from the ideal free-space case can be identified and removed, one can possibly avoid another simulation of the antenna in the ideal environment.

In post processing, the influence of scattering can be removed only if it can be identified in the measured signals in the first place. All techniques to detect scattering effects are based on matching the measured data with a-priori knowledge of the antenna.

The AUT currents are of course caused by the free-space response, but they might be also influenced by mutual coupling with scatterers in some distance. Then, the measured fields can be modeled with contributions from both the currents in the AUT volume and currents on scattering objects The currents which are due to the free-space response of the AUT usually appear before any scattering currents e.g., on a scatterer at some distance to the AUT, and the corresponding measured fields have to come from within the AUT volume. Accordingly, echo suppression techniques can be sorted into two categories: Time domain suppression techniques [1]–[9] isolate the scattering due to the delayed temporal appearance and frequency domain techniques trace the radiated fields back to their spatial origin (spatial filtering) [10]–[14] and work with single frequency data. Spatial filtering tries to fit the measurement data to a localized antenna model; this is implemented either by localized equivalent sources [10]–[12] or modal echo suppression [13], [14]. Due to the localized nature of the antenna, only a certain number of field modes are identified as belonging to the AUT and all field modes which are not radiated from within the AUT location are removed.

Time domain and frequency domain echo suppression methods have been combined successfully in the past [15], [16], but usually the measured signals are time gated before they are further processed. In this work, we reconstruct equivalent currents on a mesh enclosing the AUT for all frequencies first. The currents are then time gated based on sparse time domain reconstruction [8]. Time gating the reconstructed currents is in particular useful when the scatterers are fixed with respect to the AUT (but not limited to this case) since time gating of the measured probe signals may be unfeasible for some measurement samples. Numerical simulations verify the effectiveness and accuracy of the method even at frequencies which are close to the borders of the measured bandwidth.

II. Reconstruction and Sparse Time Gating of Equivalent Currents

We assume a measurement scenario as depicted in Fig. 1. A field probe is moved around the AUT to sense the radiated field. The radiated field in this scenario is distorted by a scatterer and for some measurement angles the probe is located in the shadow region of the scatterer. It is not possible to use

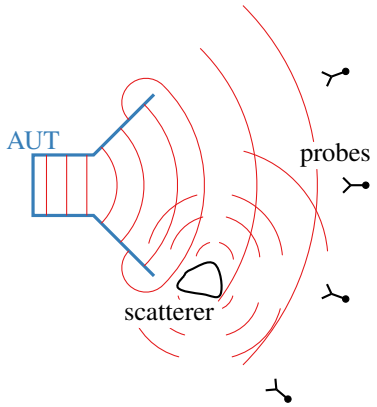

Fig. 1. Measurement scenario.

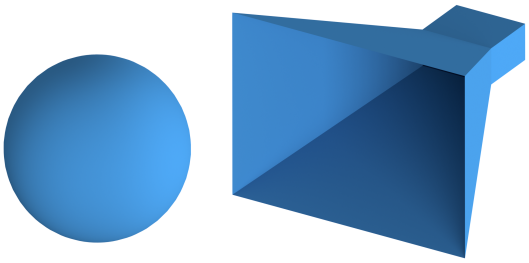

Fig. 2. Simulation setup.

time gating directly to get rid of the echo distortions for these measurement samples because the echo path is not considerably longer than the direct line of sight (LOS) path from the AUT. Therefore, we use the Fast Irregular Antenna Field Transformation Algorithm (FIAFTA) to reconstruct equivalent currents on separate surfaces enclosing both, the AUT and the scatterer first for all measured frequencies. If we obtain sufficiently many measurement samples around the AUT and the scatterer, it is possible to separate the influences of the AUT currents from the echo currents on the field. The desired free-space radiation of the AUT must have its origin within the AUT volume and we can neglect all reconstructed currents on the scatterer for further processing. However, this may not be sufficient, because the AUT currents may still be distorted from the presence of the nearby scatterer. We can only identify the undesired distortions in the AUT currents in time domain, because they appear at the same location as the desired free-space AUT currents.

In time domain, we have for every current element a sequence of impulses. We can find the amplitudes of these impulses by requesting that the Fourier transform of the impulse sequence matches with the reconstructed current coefficients in frequency domain. We expect the signal to be sparse in time domain if there is only a small number of scatterers in the proximity of the AUT. Enforcing sparsity in the time domain helps to avoid truncation effects at the band edges and can increase the accuracy of the time gated signals [8], [9]. The problem is treated as a so-called basis pursuit denoising optimization problem

$$\min_{\boldsymbol{s}_{\mathrm{TD}}} \|\boldsymbol{s}_{\mathrm{TD}}\|_1 \qquad \text{s.t.} \quad \|\boldsymbol{W}\boldsymbol{s}_{\mathrm{TD}} - \boldsymbol{s}_{\mathrm{FD}}\|_2 < \sigma\,, \tag{1}$$

where $\boldsymbol{s}_{\mathrm{TD}}$ is the time domain signal which we want to reconstruct for each current element, $\boldsymbol{s}_{\mathrm{FD}}$ is the corresponding frequency domain signal of the current element known from FIAFTA and $\boldsymbol{W}$ is a discrete Fourier transform matrix. The relaxation parameter σ can be adjusted to represent a value on the order of the noise floor. The solution is sparser for larger sigma but the deviation from the reference is also increased. In this work we use the SPGL1 solver [17], [18] to obtain the sparse time domain signal.

The time domain signal is thereafter truncated before the echo influence disturbs the current distribution on the AUT and transformed into the frequency domain with a discrete Fourier transform. The time gated currents, now available at each frequency, are used to finally determine the desired AUT far-field which is ideally identical to the free-space far-field.

III. Numerical Results

In order to investigate the capabilities of the proposed processing technique, a horn antenna with an echo obstacle in main beam direction has been simulated in Feko [19]. The simulation setup is depicted in Fig. 2. In about 0.3 m distance to the aperture of the AUT, a perfectly electrically conducting (PEC) sphere with 0.1 m radius is placed slightly asymmetrically offset from the main radiation direction. The near-field (NF) of the setup was simulated from 1.7 GHz to 5.7 GHz with a frequency step of $\Delta f = 50$ MHz on a spherical surface in 1.5 m distance from the origin in the center of the AUT.

In a first processing step, equivalent electric and magnetic currents were obtained on two hull surfaces around the horn and the sphere using FIAFTA. For the reconstruction, the closed hull surfaces were about 1 cm larger in each dimension than the mesh which was used to generate the synthetic data. When electric and magnetic currents are used as equivalent sources, the inverse problem is ambiguous. In this work, we use a combined source condition [20]–[22] to make the solution unique. The uniqueness of the solution at each frequency may be important when solutions at different frequencies are processed together, as it is the case for time gating. Figure 3 shows the retrieved co-polarized component of the ϑ-cut in the FF at 3.7 GHz before the time gating step. The deviation is calculated according to

$$\epsilon_{\mathrm{dB}} = 20\,\log\left(\frac{\left|E_{\vartheta}(\vartheta,\varphi) - E_{\vartheta,\mathrm{ref}}(\vartheta,\varphi)\right|}{E_{\mathrm{ref,max}}}\right). \tag{2}$$

Only the retrieved currents on the AUT were considered for the FF calculation. The reference was obtained from a free space simulation of the horn in Feko. This plot shows the limitations of only spatial filtering. Since the current distribution on

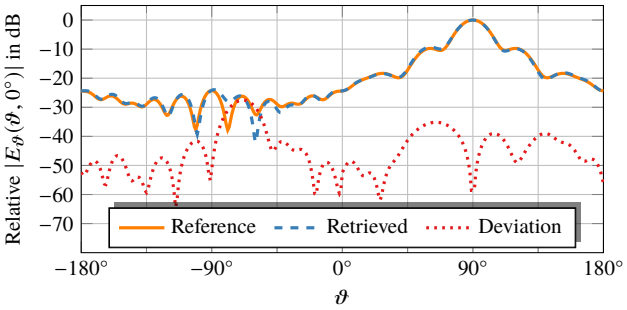

Fig. 3. Retrieved ϑ-cut of the far-field (FF) at 3.7 GHz before time gating.

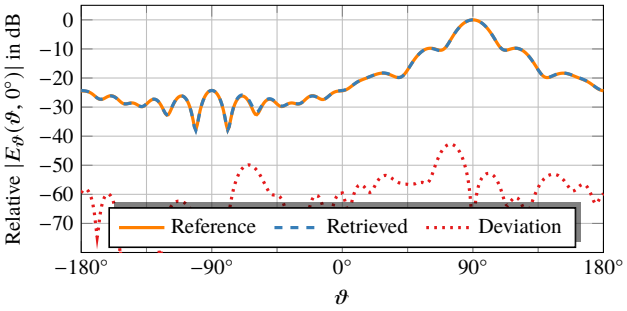

Fig. 4. Retrieved ϑ-cut of the FF at 3.7 GHz after time gating.

the AUT is altered due to the closely placed scatterer, the obtained FF deviates from the free-space fields of the horn. The deviation is worst in the backlobe direction since this is the direction of the backscattered fields which disturb the current distribution on the AUT.

In the second processing step, the currents on the sphere are neglected for further calculations and the remaining currents on the AUT mesh are time gated. For each current element the temporal impulse response has been obtained using (1) and a fixed gating window was applied for all elements. The stop time for the gating window was chosen according to the expected travelling time of the backscattered fields at 2.05 ns. This corresponds to a traveled distance of 0.61 m for a wave in vacuum (which is about double the distance between the AUT and the scatterer). The retrieved FF is shown in Fig. 4. The maximum deviation is around −42 dB, while the error is below −50 dB for most angles. The undesired echo effects on the current distribution were successfully removed.

Due to the sparse time response reconstruction not only the frequencies in the center of the measured bandwidth are cleaned from undesired contributions but also the frequencies at the edges of the measured bandwidth are reconstructed correctly. To support this claim, Fig. 5 shows the reconstructed FF at 1.9 GHz. The maximum error is around −40 dB. Although the results are not as convincing as for the center frequency, echo effects are effectively removed and the backlobe is reconstructed equally well as the rest of the FF.

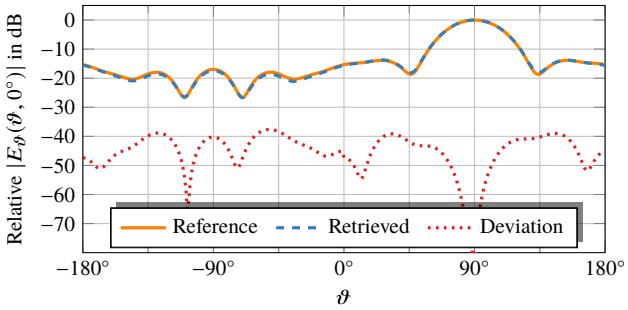

Fig. 5. Retrieved ϑ-cut of the FF at 1.9 GHz after time gating.

IV. Conclusion

For certain echoic measurement scenarios it is necessary to combine frequency domain echo suppression techniques with time gating to get rid of all undesired perturbation effects. We presented a post processing technique, which effectively combines spatial filtering and sparsity based time gating to mitigate the drawbacks of each individual method.

In the center of the measured frequency band, the free space radiation of the AUT could be reconstructed very accurately with a deviation of less than −50 dB for most angles. The proposed post processing method is useful not only in echoic measurement scenarios, but also simulation times may be reduced because the AUT can be simulated together with its environmental influences and the free space radiation can be obtained without an additional full wave simulation.

V. Acknowledgement

This work was supported in part by the Deutsche Forschungsgemeinschaft (DFG) under Grant EI 352/20-1.

References

[1] P. S. H. Leather, J. D. Parsons, and J. Romeu, "Signal processing techniques improve antenna pattern measurement," in *IEEE Antenna Measurements and SAR*, Loughborough, UK, May 2004, pp. 97–100.

[2] S. Loredo, G. Leon, S. Zapatero, and F. Las-Heras, "Measurement of low-gain antennas in non-anechoic test sites through wideband channel characterization and echo cancellation [Measurements Corner]," *IEEE Antennas and Propagation Magazine*, vol. 51, no. 1, pp. 128–135, Feb. 2009.

[3] S. Loredo, M. R. Pino, F. Las-Heras, and T. K. Sarkar, "Echo identification and cancellation techniques for antenna measurement in non-anechoic test sites," *IEEE Antennas and Propagation Magazine*, vol. 46, no. 1, pp. 100–107, Aug. 2004.

[4] M. M. Leibfritz, M. D. Blech, F. M. Landstorfer, and T. F. Eibert, "A comparison of software- and hardware-gating techniques applied to near-field antenna measurements," *Advances in Radio Science*, vol. 5, pp. 43–48, Jun. 2007.

[5] A. Henderson, J. R. James, P. Newham, and G. Morris, "Analysis of gating errors in time domain antenna measurements," in *IEE Proceedings H - Microwaves, Antennas and Propagation*, vol. 136, Aug. 1989, pp. 311–320.

[6] B. N. Levitas and D. M. Ponomarev, "Antenna measurements in time domain," in *IEEE Antennas and Propagation Society International Symposium*, vol. 1, Baltimore, USA, Jul. 1996, pp. 573–576 vol.1.

[7] R. V. De Jough, M. Hajian, and L. P. Ligthart, "Antenna time-domain measurement techniques," *IEEE Antennas and Propagation Magazine*, vol. 39, no. 5, pp. 7–11, Oct. 1997.

[8] R. A. M. Mauermayer and T. F. Eibert, "Time gating based on sparse time domain signal reconstruction from limited frequency domain information," in *Antenna Measurement Techniques Association (AMTA) Annual Symposium*. Austin, TX, USA: IEEE, Oct. 2016, pp. 1–4.

[9] ——, "Sparse time domain signal representation for echo suppression in antenna measurements," in *2017 International Conference on Electromagnetics in Advanced Applications (ICEAA)*. IEEE, Sep. 2017, pp. 1247–1249.

[10] J. L. A. Quijano, L. Scialacqua, J. Zackrisson, L. J. Foged, M. Sabbadini, and G. Vecchi, "Suppression of undesired radiated fields based on equivalent currents reconstruction from measured data," *IEEE Antennas and Wireless Propagation Letters*, vol. 10, pp. 314–317, Apr. 2011.

[11] F. Cano-Facila, S. Burgos, F. Martin, and M. Sierra-Castaner, "New reflection suppression method in antenna measurement systems based on diagnostic techniques," *IEEE Transactions on Antennas and Propagation*, vol. 59, no. 3, pp. 941–949, Dec. 2011.

[12] J. Kornprobst, A. Paulus, T. F. Eibert, and R. A. M. Mauermayer, "Method-of-Moments modeling of conducting objects within the fast irregular antenna field transformation algorithm," San Diego, CA, USA, Oct. 2019.

[13] D. Hess, "The IsoFilter™ technique: a method of isolating the pattern of an individual radiator from data measured in a contaminated environment," *IEEE Antennas and Propagation Magazine*, vol. 52, no. 1, pp. 174–181, Feb. 2010.

[14] S. F. Gregson, A. C. Newell, and G. E. Hindman, "Reflection suppression in cylindrical near-field antenna measurement systems–cylindrical MARS," in *Antenna Measurement Techniques Association (AMTA) Annual Symposium*, Salt Lake City, UT, USA, Nov. 2009.

[15] J. Knapp and T. F. Eibert, "Near-field antenna pattern measurements in highly reflective environments," *IEEE Transactions on Antennas and Propagation*, vol. 67, no. 9, pp. 6159–6169, Sep. 2019.

[16] J. Knapp, J. Kornprobst, and T. F. Eibert, "Equivalent source and pattern reconstruction from oversampled measurements in highly-reflective environments," *IET Microwaves, Antennas & Propagation*, Jun. 2019.

[17] E. van den Berg and M. P. Friedlander, "Probing the pareto frontier for basis pursuit solutions," *SIAM Journal on Scientific Computing*, vol. 31, no. 2, pp. 890–912, Jan. 2009.

[18] M. Friedlander and E. Van den Berg, "SPGL1: A solver for large-scale sparse reconstruction," *SIAM Journal on Scientific Computing*, vol. 31, no. 2, pp. 890–912, Jun. 2008.

[19] Altair, "Feko." [Online]. Available: https://altairhyperworks.com/

[20] T. F. Eibert, D. Vojvodic, and T. B. Hansen, "Fast inverse equivalent source solutions with directive sources," *IEEE Transactions on Antennas and Propagation*, vol. 64, no. 11, pp. 4713–4724, Nov. 2016.

[21] J. Kornprobst, R. A. Mauermayer, O. Neitz, J. Knapp, and T. F. Eibert, "On the solution of inverse equivalent surface-source problems," *Progress In Electromagnetics Research*, vol. 165, pp. 47–65, 2019.

[22] T. B. Hansen, A. Paulus, and T. F. Eibert, "On the condition number of a normal matrix in near-field to far-field transformations," *IEEE Transactions on Antennas and Propagation*, vol. 67, no. 3, pp. 2028–2033, Mar. 2019.